Journal of Nuclear Materials 481 (2016) 46–52

Contents lists available at ScienceDirect

Journal of Nuclear Materials

journal homepage: www.elsevier.com/locate/jnucmat

Interactions between displacement cascades and Σ3⟨110⟩ tilt grain boundaries in Cu

Bo Li [a, c], Xiao-Jiang Long [c, d], Zhao-Wu Shen [a, **], Sheng-Nian Luo [b, c, *]

[a] CAS Key Laboratory of Mechanical Behavior and Design of Materials, Department of Modern Mechanics, University of Science and Technology of China, Hefei, Anhui, 230027, PR China
[b] Key Laboratory of Advanced Technologies of Materials, Ministry of Education, Southwest Jiaotong University, Chengdu, Sichuan, 610031, PR China
[c] The Peac Institute of Multiscale Sciences, Chengdu, Sichuan, 610031, PR China
[d] College of Physical Science and Technology, Sichuan University, Chengdu, Sichuan, 610064, PR China

ARTICLE INFO

Article history:
Received 25 June 2016
Received in revised form
5 September 2016
Accepted 9 September 2016
Available online 10 September 2016

Keywords:
Cascades
Grain boundary
Defects
Migration

ABSTRACT

With large-scale molecular dynamics simulations, we investigate systematically the interaction of displacement cascades with a set of Σ3⟨110⟩ tilt grain boundaries (GBs) in Cu bicrystals at low ambient temperatures, as regards irradiation-induced defect production/absorption and GB migration/faceting. Except for coherent twin boundary, GBs exhibit pronounced preferential absorption of interstitials, which depends on initial primary knock-on atom distance from GB plane and inclination angle. GB migration occurs when displacement cascades overlap with a GB plane, as induced by recrystallization of thermal spike, and concurrent asymmetric grain growth. Faceting occurs via expanding coherent twin boundaries for asymmetric GBs.

1. Introduction

One of the key challenges in nuclear engineering is designing radiation-tolerant materials. Materials during service are inevitably situated in harsh environment, including high temperature and high neutron dose [1,2]. Incident energetic neutrons produce point defects (interstitials and vacancies) [3–8], which migrate, aggregate, and eventually cause degradation of materials integrity and performance [9–12]. Therefore, developing materials that can sustain extreme radiation has been of continued interest.

Experimental investigations on nano-crystalline materials containing high density grain boundaries (GBs) have shown improved radiation resistance [5–7,13]. GBs can be sinks for internal defects, contributing to improvement in irradiation damage [5–7,13–15]. Understanding defect production and evolution near GBs, and the interactions between defects and GBs, is prerequisite for designing radiation-tolerant materials, and numerous studies have been devoted to this subject [15–28]. For example, Tschopp *et al.* [18] and Yu *et al.* [19] investigated energetics of defects interacting with different GB types in Fe and Cu, and reported pronounced reduction of interstitial formation energy within several-layer distance from GBs. Samaras *et al.* found that GBs act as sinks for interstitials [15–17]. Bai *et al.* observed defect annihilation via a "loading-unloading" mechanism and preferential absorption of interstitials near GBs (as opposed to vacancies) [20,22]. Han *et al.* claimed that GB sink efficiency depends on all GB characters [27]. Other materials investigated include W [24], Zr [25] and Mo [28]. Eventually, it is worthwhile to investigate displacement cascades near other types of GBs, since its evolution varies with materials and GB types.

Moreover, both experiments and molecular dynamics (MD) simulations have shown that radiation-induced GB migration and grain growth can occur in nano-crystalline materials [29–39]. Yu *et al.* ascribed GB migration to dislocation loop-GB interactions and defects absorption [39]. Li *et al.* inferred that GB migrates through collective glide Shockley dislocations driven by absorbed interstitials [40]. Yu *et al.* found that GB can migrate under successive vacancy injecting [41]. Low temperature (or "nonthermal") grain growth was also predicted when a thermal spike overlaps with GBs [32–34]. Voegeli *et al* reported that grain growth induced by ion-

* Corresponding author. Key Laboratory of Advanced Technologies of Materials, Ministry of Education, Southwest Jiaotong University, Chengdu, Sichuan, 610031, PR China.
** Corresponding author.
E-mail addresses: ZWShen@ustc.edu.cn (Z.-W. Shen), sluo@pims.ac.cn (S.-N. Luo).

http://dx.doi.org/10.1016/j.jnucmat.2016.09.011
0022-3115/

beam irradiation is a direct result of recrystallization of thermal spikes and fundamentally different from that due to thermal annealing [33]. Kaoumi *et al* proposed a thermal spike model to describe grain growth under irradiation, where GB migration is achieved by atom jumps within the thermal spike [34]. Despite the high probability of collision cascades being initiated on GBs in nano-crystalline materials, studies along this line are rare, and very limited evolution details are available.

Since the evolution of primary irradiation damage is on pico-second time scale, MD simulations are appropriate for acquiring microscopic information. In this work, we perform a systematic study on the interactions of displacement cascades with a set of Σ3 ⟨110⟩70.53° tilt GBs in Cu, a model system for face-centered-cubic (FCC) metals widely used in the studies of irradiation damage [42–46]. We explore the effects of the initial distance of the primary knock-on atom (PKA) from a GB plane, as well as the inclination angle (ϕ), on the survivability of point defects in the bulk region. Low temperature GB migration is investigated along with its mechanism. Section 2 addresses the methodology of MD simulations and data analysis, followed by results and discussions in Sec. 3, and concluding remarks in Sec. 4.

2. Methods

The Large-scale Atomic/Molecular Massively Parallel Simulator (LAMMPS) [47] is employed for our MD simulations, along with an accurate embedded-atom-method (EAM) potential of Cu [48]. This widely used EAM potential has well established accuracy in describing, e.g., defect formation energy, stacking fault energy and melting point [48,49]. When the interatomic distance is smaller than 0.5 Å, this EAM potential is smoothly splined to the Ziegler-Biersack-Littmark (ZBL) potential [50,51].

We investigate a group of Σ3⟨110⟩ tilt GBs with identical misorientation angle 70.53°. Among those GBs, two GBs are symmetric tilt grain boundaries, namely coherent twin boundary (CTB) and symmetric incoherent tilt boundary (SITB). Other GBs are asymmetric tilt GBs (ATGBs) with different inclination angle (ϕ) relative to CTB, ranging from 0° to 90°. Therefore, ϕ=0° and 90° for CTB and SITB, respectively. Details for constructing such bicrystals and crystallographic orientations of constituent grains were presented previously [52]. The tilt axis [011] is the *x*-axis, the GB normals are along the *z*-axis, and the *y*-axis is on the GB plane orthogonal to the *x*- and *z*-axes (Fig. 1). The dimensions of a bicrystal are about 80 × 20 × 53 nm^3, corresponding to a system size of ~7 million atoms. The as-constructed bicrystals are relaxed with the conjugate gradient method and thermalized at the ambient conditions with the constant-pressure-temperature ensemble and three-dimensional (3D) periodic boundary conditions. After equilibration, ATGBs exhibit multiple alternating CTB and SITB segments. For ϕ>70.53°, the total length of CTB segments decreases to nearly zero, while the 9R phase emits from the GB plane.

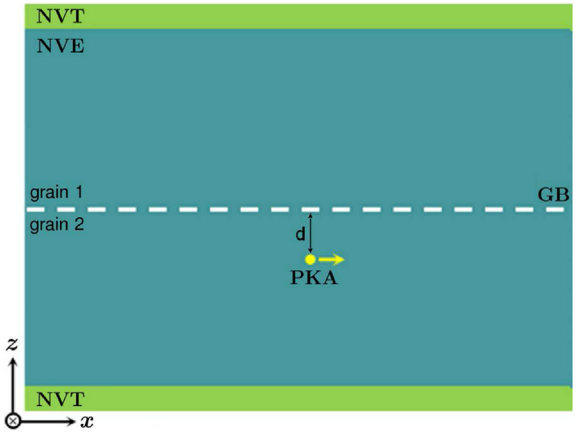

Fig. 1. Schematic configuration of MD cascade simulations.

PKA with a recoil energy of 5 keV is introduced into the system via assigning an equivalent velocity to an atom. To reduce the difference among simulations as much as possible, the PKA directions are all along the tilt axis ⟨110⟩, namely, parallel to the GB plane. The initial distance (*d*) of PKA from a GB plane is defined as the difference in the *z*-coordinates of PKA and the GB plane. Negative *d*-values mean that PKA is located below a GB plane. For each irradiation case, at least ten MD runs with randomly assigned PKA positions are carried out. The time step for integrating the equation of motion is 0.005 fs initially, and then increases to 1 fs as long as no atoms are displaced by more than 0.05 Å within a single time step. The total run durations are up to 50 ps. During cascade simulations, the canonical ensemble (*NVT*) is applied to the outmost, 25 Å thick, layers along the *z*-axis, in order to achieve an isothermal environment in the far field, while the microcanonical ensemble (*NVE*) is used for the remaining region with the cascade [24,25] (Fig. 1). To mimic "nonthermal" irradiation as commonly investigated in literature [53,54], the temperature of thermostat in the *NVT* region is set to 10 K.

Voronoi tessellation method is applied to estimate individual atom volume for calculating atomic stresses [55]. Visualization and partial post-processing are performed using a software package OVITO [56]. An algorithm based on the Wigner-Seitz cell is utilized to characterize interstitials and vacancies [57,58]. For the analysis of point defects, only the defects in the bulk region (excluding the GB region) are counted as surviving ones. Common neighbor analysis is also adopted to characterize local structures [57], including FCC, body-centered cubic (BCC), and hexagonal close-packed (HCP) types, and other types.

3. Results and discussion

3.1. Production of point defects near a GB plane

We investigate the changes in the number of surviving defects in the bulk region during a period of several ps after introducing PKA, as a function of the initial distance of PKA from a GB plane, and the inclination angle of the grain boundary. Here, the number of surviving defects, n_s, is defined as the number of point defects subtracted by the number of Frenkel pairs produced in a single crystal from cascading at the same PKA direction and energy.

We take the case of ϕ=19.47° as an example to elucidate the dependence of n_s on the initial PKA distance, *d*. The results are shown in Fig. 2. Given the asymmetry of ATGBs, their $n_s(d)$ curves for the defects in the bulk region are also asymmetric about the *xy*-plane (*d*=0 Å). Within a 40 Å distance from the GB plane, interstitial absorption ($n_s \leq 0$) occurs: the number of surviving interstitials in the bulk region is smaller than that produced in a corresponding single crystal. The $n_s(d)$ curves of surviving vacancies are typically M-shaped, with a minimum value at *d*=0 Å. Since the PKA incident direction is parallel to the GB plane, overlapping of a cascade with the GB region peaks at *d*=0 Å. Hence, most vacancies are directly created in the GB region, but are excluded from counting as surviving vacancies, resulting in the dip at *d*=0. With increasing *d*, the overlapping between a cascade and GB decreases, and more vacancies are created in the bulk region. So the number of surviving vacancies in grain interiors increases; n_s for vacancies reaches the maximum at $|d| = 20$ Å. That is the critical distance where the